Journal of Alloys and Compounds 513 (2012) 91–96

Contents lists available at SciVerse ScienceDirect

Journal of Alloys and Compounds

journal homepage: www.elsevier.com/locate/jallcom

Effects of Cr_2O_3 addition on the mechanical properties, microstructure and wear performance of zirconia-toughened-alumina (ZTA) cutting inserts

Ahmad Zahirani Ahmad Azhar[a], Lee Chun Choong[a], Hasmaliza Mohamed[a], Mani Maran Ratnam[b], Zainal Arifin Ahmad[a,*]

[a] School of Materials and Mineral Resources Engineering, Engineering Campus, Universiti Sains Malaysia, 14300 Nibong Tebal, Pulau Pinang, Malaysia
[b] School of Mechanical Engineering, Engineering Campus, Universiti Sains Malaysia, 14300 Nibong Tebal, Pulau Pinang, Malaysia

ARTICLE INFO

Article history:
Received 10 May 2011
Received in revised form
27 September 2011
Accepted 29 September 2011
Available online 20 October 2011

Keywords:
Powder metallurgy
Oxide materials
Mechanical properties
Microstructure

ABSTRACT

The effects of Cr_2O_3 addition on microstructure, the mechanical properties and wear performance of ZTA were investigated. The powders of alumina, yttria partially stabilized zirconia and chromia were mixed and uniaxially pressed into rhombic cutting tool inserts and subsequently sintered at 1600 °C for 4 h in air. The effects of the cutting tool inserts' microstructures on their mechanical properties and wear performance were carried out. The microstructural observations show that the Al_2O_3 grain size is significantly dependent on the amount of Cr_2O_3 additives used. The Vickers hardness and fracture toughness tests are directly related to the results of wear area, where the cutting insert with the minimum wear area also showed the highest hardness and fracture toughness. The results show that an addition of 0.6 wt% of Cr_2O_3 produces the minimum wear area. ZTA cutting inserts fabricated with Cr_2O_3 additives show an increase of 26% in wear resistant capability.

1. Introduction

The excellent properties of ceramics have made it a good candidate for cutting insert applications, especially in high temperature and high speed conditions [1]. Alumina based materials are one of the most popular ceramics used to make cutting inserts as it has high hot hardness, high abrasion resistance and chemical inertness against the environment and the workpiece. Therefore, alumina based materials are always used in abrasive wear environments such as coal chutes, ball mills, grinders and mixers [2]. Unfortunately, alumina based cutting inserts have low toughness and cause failures such as chipping and breakage during machining [3]. As a result, secondary materials such as yttria stabilized zirconia (YSZ) [4], titanium carbide, silver and ceria are used to improve the fracture toughness of alumina [5,6].

Zirconia-toughened-alumina (ZTA) has been another recent addition to the repertoire of high performance ceramics. The ZTA composite was developed to substitute alumina ceramics in applications where a higher fracture resistance is required, for the phase transformation from the tetragonal phase to the monoclinic phase [3,4,7–10]. Even though with the reinforcement of YSZ, the properties of fracture toughness of ZTA only improved to ~4.5 MPa $m^{1/2}$ compared to monolithic Al_2O_3: 3.9 MPa $m^{1/2}$ [8]. Thus, the performance of a ZTA cutting insert is limited by its fracture toughness. In order to further improve ZTA cutting insert performance, the fracture toughness needs to be improved.

Chromia (Cr_2O_3) is one of the many additives potentially able to improve the physical properties of alumina. When chromia is added into an alumina system, isovalent solid solution will form over the full range of compositions due to the fact that both chromia and alumina are sesquioxides and have the same corundum crystal structure (approximately hexagonal close-packed oxide ions with the Al^{3+} and Cr^{3+} ions occupying two thirds of the available octahedral intertitials sites). In reactions at high temperatures (T > 1000 °C), complete ranges of substitution solid solutions are obtained [11–13]. Isovalent solid solution happens when an atom or ion replaces an atom or ion of the same charge in the parent structure. It contributes to high refractoriness and chemical stability [12]. The addition of Cr_2O_3 also increases the hardness, tensile strength and thermal shock resistance of alumina [14]. When a small amount of Cr_2O_3 (~2 mol%) is added, the grains become larger and bimodal in size distribution. At the same time, the fracture toughness and flaw tolerance of alumina are also improved. The hardness as well as elastic modulus is increased. However, fracture strength decreases with the addition of Cr_2O_3 [14].

Even though the study of ZTA and Al_2O_3–Cr_2O_3 has been done extensively for the past 20 years, the studies were carried out individually. In this study, the microstructural evolution, mechanical properties and wear performances of Cr_2O_3 doped ZTA were

* Corresponding author. Tel.: +60 012 6671736; fax: +60 04 594 1011.
E-mail address: zainal@eng.usm.my (Z.A. Ahmad).

0925-8388/$ – see front matter © 2011 Elsevier B.V. All rights reserved.
doi:10.1016/j.jallcom.2011.09.092

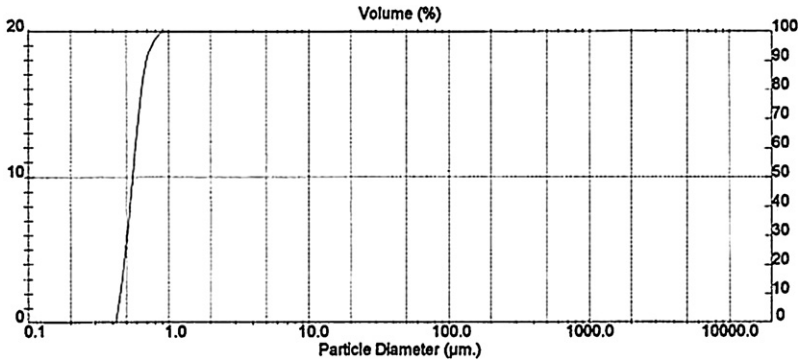

Fig. 1. Particle size of Cr_2O_3.

investigated and the influence of Cr_2O_3 addition on its microstructure and mechanical properties were discussed.

2. Experimental work

Monolithic Al_2O_3 (average particle size 0.5 μm, supplier Martinswerck, 99% purity), YSZ (average particle size 1.5 μm, supplier Goodfellow (ZR616010), with 5.4 wt% Y_2O_3 as stabilizer) and Cr_2O_3 (average particle size 0.5 μm, supplier Sigma–Aldrich, 99.9% purity) were used as the starting materials. Ceramic cutting inserts with an average of 0.60 mm tip radius were fabricated via the solid state processing route. Samples with an 80/20 ratio for Al_2O_3/YSZ respectively were prepared with different Cr_2O_3 wt% ranging from 0 wt% to 1.0 wt%.

The powders were wet mixed for 30 min using ultrasonic machine (JAC 1002, KODO Technical Research Co., Ltd., Japan) and automatic stirrer (Automatic Heidolph RZR 2041). Subsequently, the mixture was dried for 24 h in an oven at 100 °C. The powders of Al_2O_3, YSZ and Cr_2O_3 were then mixed with 0.6 wt% of polyethylene glycol 400 using a ball mill for 8 h. The composite powder now was uniaxially pressed into rhombic cutting inserts at 295 MPa using a hydraulic press. The specimens were then sintered in a HTF 1800 Carbolite furnace at 1600 °C for 4 h in air, with 5 °C min^{-1} sintering rate for both heating and cooling rate (furnace cooled). ISO specification for turning tool holder and the turning process is based on ISO 3685.

Properties such as density, Vickers hardness and fracture toughness were measured. Fracture toughness was calculated using the formula proposed by Niihara [15] for Palmqvist crack. Value for Young Modulus (E) used in this study is 310 GPa. Surface cracks generated by Vickers indentation can be used to calculate the fracture toughness of brittle materials such as ceramics and glasses. A mathematical model proposed by Niihara has been taken into consideration for determining the fracture toughness of the samples. This technique employs a sharp indenter to grow cracks in a material at the microstructural level. The length of these cracks can then be used to calculate the toughness of the material using an empirical relation. Indentation fracture toughness has some major advantages over traditional toughness testing methods; it allows measurement at the microscale, no need for machining microspecimens, efficient and allowing many measurements on a small quantity of material.

$$3K_{1c} = 0.035(\mathrm{Ha}^{1/2})\left(\frac{3E}{H}\right)^{0.4}\left(\frac{l}{a}\right)^{-0.5} \quad (1)$$

whereas K_{1c} is the fracture toughness, H is Vickers hardness, a is the half length of Vickers diagonal (μm), E is equal to the Young modulus of the samples and l is the length of the radial crack size (μm).

Field emission scanning electron microscopy (FESEM) was used to study the microstructure of the sintered samples. The samples were thermally etched in the same furnace used for sintering at 1400 °C for 2 h.

XRD of the sintered cutting insert was carried out to determine the phases present. The XRD patterns of the sintered products were obtained using a Bruker D8 Advanced operated in Bragg–Brentano geometry, with Cu Kα radiation, in the $10^\circ \le 2\theta^\circ \le 90^\circ$ range. Counting time was fixed at 71.5 s for each 0.03° 2θ step. The X-ray tube was operated at 40 kV and 30 mA. Quantitative phase analysis was measured by Rietveld method using HighScorePlus software. Crystal structure data for each phase present in the samples were taken from ICSD. The refinement was done in stages, with the atomic coordination and thermal parameters held fixed.

Wear analysis were carried out by capturing the images of the cutting tips before and after machining. The turning process was done on a lathe machine Hurricane 600. Table 1 shows the machining parameter used for this study. A high-resolution CCD camera (Model: JAI CV-A1, resolution 1296 × 1024 pixels) fitted with a 50 mm lens and a 110 mm extension tube was used to capture the image of the cutting tip. Backlighting was used to highlight the profile of the tool. The field-of-view of the CCD camera is 2.3 mm × 2 mm, and the distance from the front end of camera lens to the cutting tool is approximately 60 mm. An algorithm using Wiener filtering, median filtering, morphological operations and thresholding was developed using MatLab to calculate wear area. Detailed processing route, characterization techniques, machining parameter and wear area measurement are described elsewhere [16]. In addition, the flank wear of the cutting insert were also observed after the turning process. Flank wear at each turning run was measured by an optical microscope.

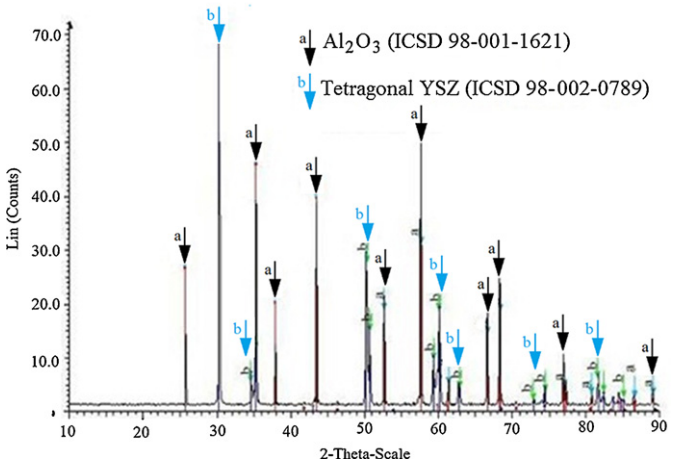

Fig. 2. XRD results of addition of 0.5 wt% of Cr_2O_3 into ZTA cutting insert after the sintering process which (a) represent tetragonal alumina corundum (ICSD reference 98-001-1621) and (b) represent the tetragonal yttria stabilized zirconia (ICSD reference 98-002-0789).

3. Results and discussion

Fig. 1 shows that the median particle size (d_{50}) of Cr_2O_3 is 0.66 μm and 99% of the particles are less than 0.92 μm. The Cr_2O_3 was in the corundum phase and matched with the ICSD reference 98-005-6901. XRD results for the sintered ZTA–Cr_2O_3 cutting inserts are shown in Fig. 2. XRD analysis indicates that Al_2O_3 was present as corundum (ICSD reference 98-001-1621). XRD analysis also showed that YSZ has tetragonal crystal structures together with the presence of yttria (ICSD reference 98-002-0789). There is no monoclinic ZrO_2 phase observed. On the other hand, the XRD result does not detect the presence of Cr_2O_3 phase in the sample.

Table 1
Machining parameters.

Parameters	Value
Cutting speed (RPM)	540
Depth of cut (mm)	0.80
Feed rate (mm/rev)	0.2
Workpiece	316 stainless steel
Workpiece diameter (mm)	12.70
Cutting environment	Dry

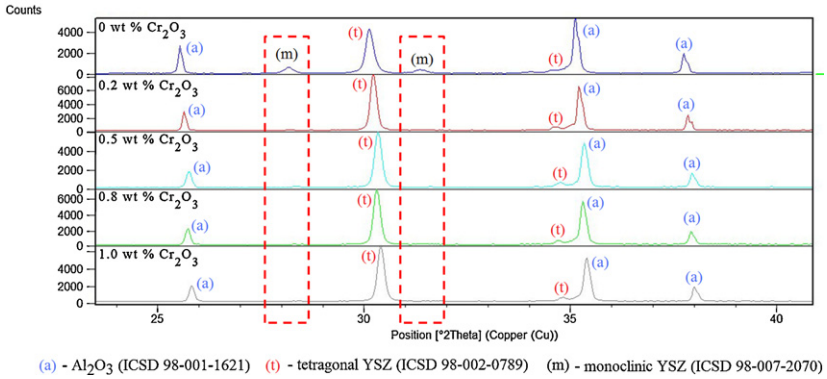

Fig. 3. Comparison of XRD results for ZTA cutting insert with various addition of Cr_2O_3 wt%.

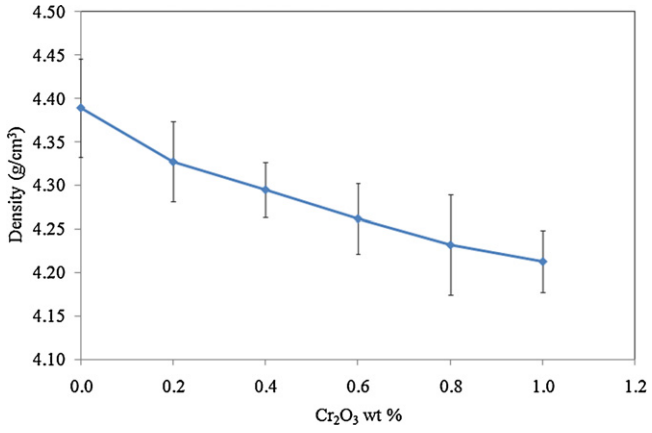

Fig. 4. Density of ZTA–Cr_2O_3 cutting inserts as a function of Cr_2O_3 wt%.

According to the XRD analysis no new compound was formed with the addition of Cr_2O_3. Fig. 3 shows the comparison of XRD results of ZTA samples with various Cr_2O_3 wt%. It is shown that the addition of Cr_2O_3 would result the monoclinic phase to disappear (shown in the red dotted box), whereas the peaks for monoclinic phase are no longer seen for samples of ZTA with the addition of Cr_2O_3. Table 2 shows the effect of Cr_2O_3 addition to the lattice parameter of Al_2O_3. It is increased from 4.757754 Å to 4.761456 Å and from 12.990660 Å to 13.003890 Å for lattice parameter *a* and *c*, respectively. This increment is due to the bigger radii of Cr compare to Al.

Densities of the sintered cutting inserts were determined using the Archimedes principle. Fig. 4 shows the results of densities of the ZTA–Cr_2O_3 cutting inserts with different Cr_2O_3 wt%. The density of cutting inserts decreased from 4.38 g/cm^3 to 4.23 g/cm^3, for samples with 0 Cr_2O_3 wt% to 1.0 Cr_2O_3 wt%, respectively. This may be explained by the vaporization and condensation of Cr_2O_3 during sintering in air. Therefore, the presence of Cr_2O_3 in an alumina matrix prevents the densification process [11,17,18]. Fig. 5 shows the results of percentage of porosity for ZTA–Cr_2O_3 cutting inserts with different Cr_2O_3 content. Percentage of porosity was increased from 0.75% to 1.47%, for samples with 0 Cr_2O_3 wt% to 1.0 Cr_2O_3 wt%, respectively. This is because as the Cr_2O_3 wt% increases, the effect of vaporization and condensation of Cr_2O_3 becomes more significant in the sample [11,17,18].

Table 2
Unit cell dimension of Al_2O_3 with various Cr_2O_3 wt%.

Materials	*a* (Å)	*c* (Å)
Al_2O_3 pure	4.757754	12.990660
ZTA + 0 Cr_2O_3 wt%	4.758206	12.993020
ZTA + 0.2 Cr_2O_3 wt%	4.759128	12.984950
ZTA + 0.5 Cr_2O_3 wt%	4.758103	12.999820
ZTA + 0.8 Cr_2O_3 wt%	4.760283	13.001680
ZTA + 1.0 Cr_2O_3 wt%	4.761456	13.003890

FESEM micrographs for the polished surface of the cutting inserts are shown in Fig. 6. Consistent with previous studies, YSZ and Al_2O_3 grains are well distributed among each other but minor agglomeration was unavoidable [4,19]. EDX analysis in Fig. 7 indicates the white areas as representing YSZ grains and the dark areas as representing Al_2O_3 grains. In general, similar microstructural characteristic were observed in these samples, i.e. uniformly sized grains with high degree of grain close packing. Almost no abnormal grain growth was observed. Furthermore, few of the dark grains (Al_2O_3) grew with the increase of the Cr_2O_3 wt%. This can be seen from the micrographs by comparing the microstructure with 0 wt% Cr_2O_3 with the microstructure with 1.0 wt% of Cr_2O_3. This proved that Cr_2O_3 had accelerated the growth of alumina grains. A similar observation was recorded in the study of Riu et al. [14], which stated that the average size of grains containing Cr_2O_3 increased compared to the pure ZTA specimen. In Fig. 6, the presence of Cr_2O_3 grains cannot be seen due to the very low amount of Cr_2O_3 wt% added. However, the presence of Cr^{3-} can be proven based on the EDX results in Fig. 6(e). EDX analysis clearly shows the presence of Cr^{3-} in the cutting inserts although no grain of Cr_2O_3 is found in the micrograph. When a higher amount of Cr_2O_3 is added, the grains grow and become relatively larger compared to the grains of pure ZTA.

Fig. 8 shows the results of Vickers hardness of ZTA–Cr_2O_3 cutting inserts with various wt% of Cr_2O_3 added (*Y*-error bar indicates the standard deviation value). Based on the results, cutting inserts with 0.6 wt% of Cr_2O_3 had the optimum composition that showed

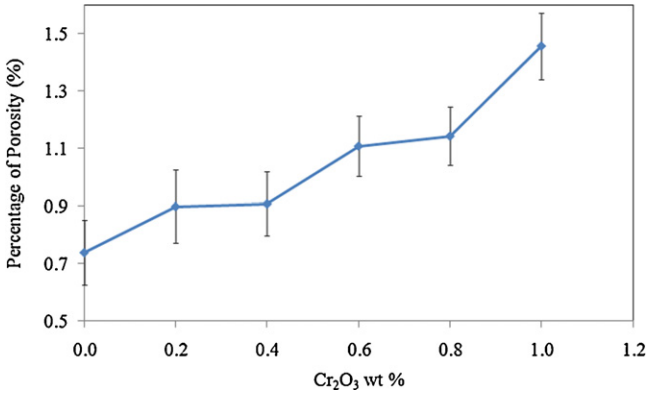

Fig. 5. Percentage of porosity for ZTA–Cr_2O_3 cutting inserts as a function of Cr_2O_3 wt%.

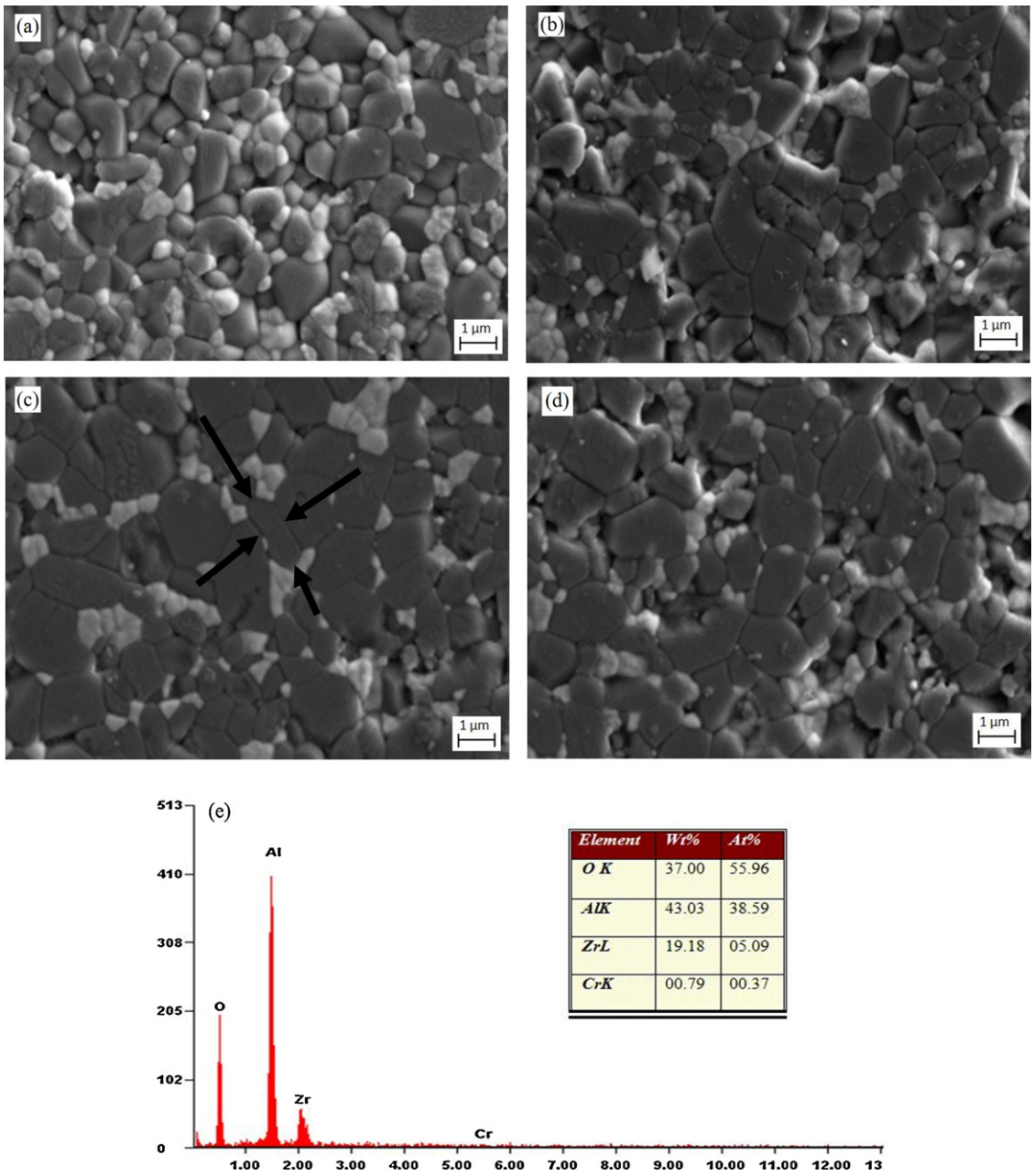

Fig. 6. Microstructural images of ZTA–Cr_2O_3 cutting inserts with addition of (a) 0 wt% Cr_2O_3, (b) 0.3 wt% Cr_2O_3, (c) 0.6 wt% Cr_2O_3, (d) 0.9 wt% of Cr_2O_3 and (e) EDX results for ZTA–Cr_2O_3 cutting insert which containing 0.8 wt% Cr_2O_3. All micrographs were taken with 5000× magnification.

highest Vickers hardness (1683 HV) among all compositions. From the micrographs (Fig. 6), the increase of hardness from 0 wt% Cr_2O_3 to 0.6 wt% Cr_2O_3 may be caused by the formation of the isovalent solid solution between Al^{3-} and Cr^{3-} as both of them (Al_2O_3 and Cr_2O_3) have the same corundum structure. The hardness of ZTA–Cr_2O_3 is higher than pure ZTA in the study of Azhar et al. [3] and has the same trend as the work done by Riu et al. [14]. With further addition of Cr_2O_3, the hardness value decreased from 0.6 wt% Cr_2O_3 to 1.0 wt% of Cr_2O_3, from 1680 HV to 1669 HV respectively. This is due to the presence of more porosity inside the samples, which is increased to 1.1% for samples with 0.6 wt% Cr_2O_3.

Fig. 9 indicates the results of fracture toughness of ZTA–Cr_2O_3 cutting inserts with various Cr_2O_3 wt% (*Y*-error bar indicates the standard deviation value). The cutting insert containing 0.6 wt% Cr_2O_3 showed maximum fracture toughness (4.73 MPa $m^{1/2}$) compared to other cutting inserts. The increase of fracture toughness is mainly caused by the crack bridging due to large grains formed which can be observed in Fig 6. The previous study conducted by Riu et al. [14] concluded that the increase of fracture toughness is due to the formation of large elongated or platelike grains in the microstructure, which can be observed in Fig. 6(c). Large grains formed due to the addition of Cr_2O_3 resulted in higher toughness and provide more resistivity to crack propagation. Addition of 0.7 wt% Cr_2O_3 onwards show decrease of fracture toughness, while with the addition of more than 1 wt% Cr_2O_3, the fracture toughness decreased to the level of the undoped specimen. This is due to the presence of pores inside the sample as a result of vaporization and condensation of Cr_2O_3 in pressureless sintering [11,17,18].

Images of the cutting tips before and after machining were captured as shown in Fig. 10. These two images were aligned automatically before subtraction. The software subsequently produced images shown in Fig. 10(a) and (b) depending on the final condition

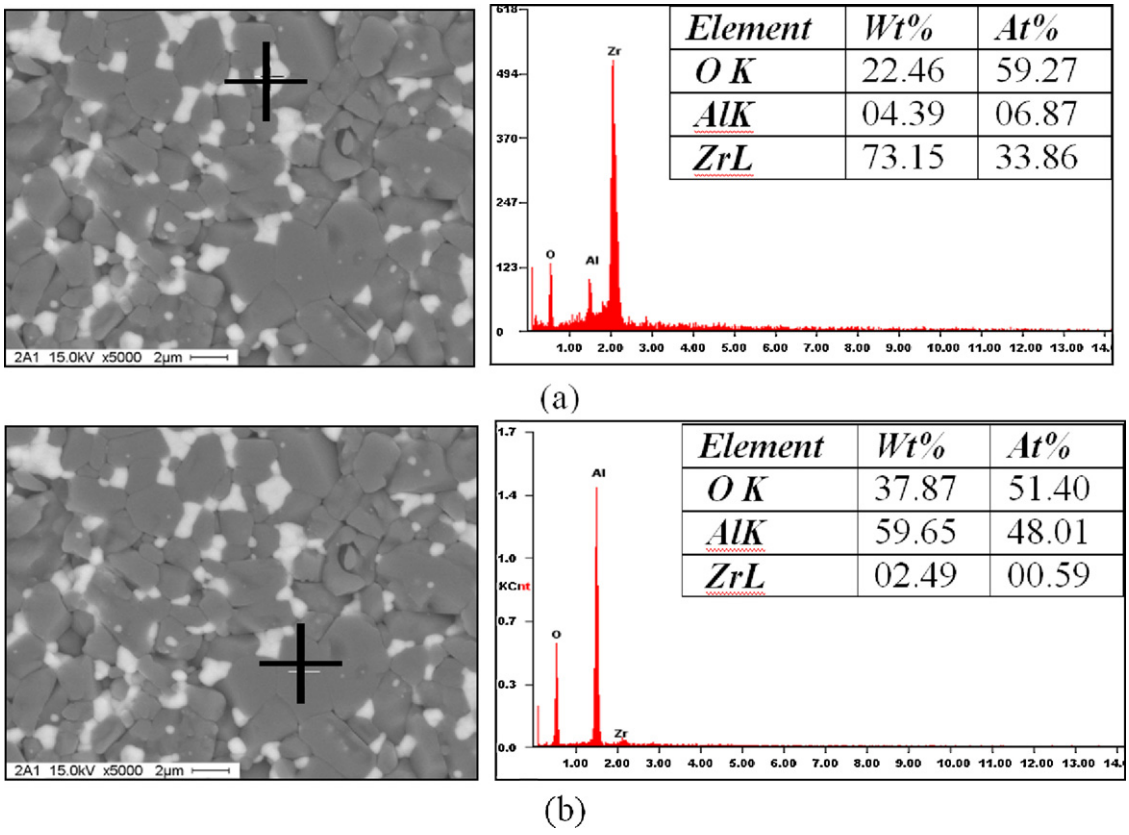

Fig. 7. EDX analysis for (a) Al_2O_3 and (b) YSZ grains.

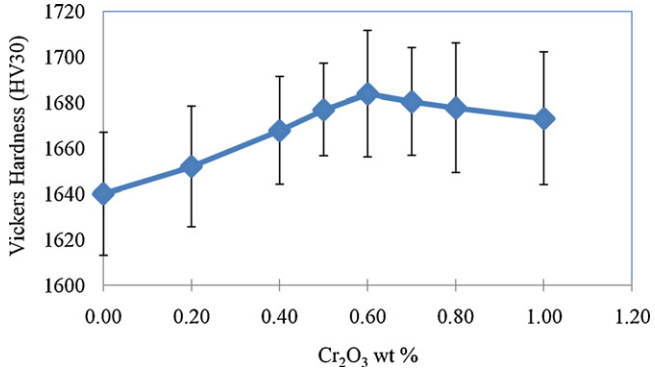

Fig. 8. Vickers hardness of ZTA–Cr_2O_3 cutting inserts as a function of Cr_2O_3 wt%.

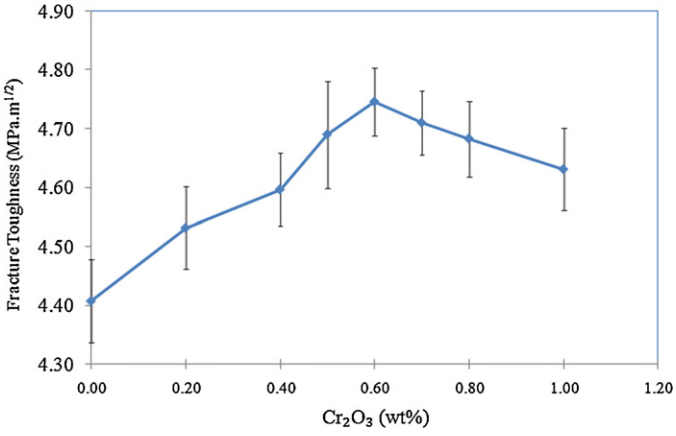

Fig. 9. Fracture toughness of ZTA–Cr_2O_3 cutting inserts as a function of Cr_2O_3 wt%.

of the inserts. Moreover, the software is able to exactly calculate the area differences between the two images, which are indicated by the black colored area in Fig. 10(c) and (d). A larger black area indicates that the inserts have experienced a greater amount of wear, i.e. more material loss has occurred due to machining.

Fig. 11 shows the wear area of ZTA–Cr_2O_3 cutting inserts with various Cr_2O_3 content (*Y*-error bar indicates the standard deviation value), respectively. Only the cutting inserts with 0.5 wt% Cr_2O_3, 0.6 wt% Cr_2O_3 and 0.7 wt% Cr_2O_3 were tested for machining since

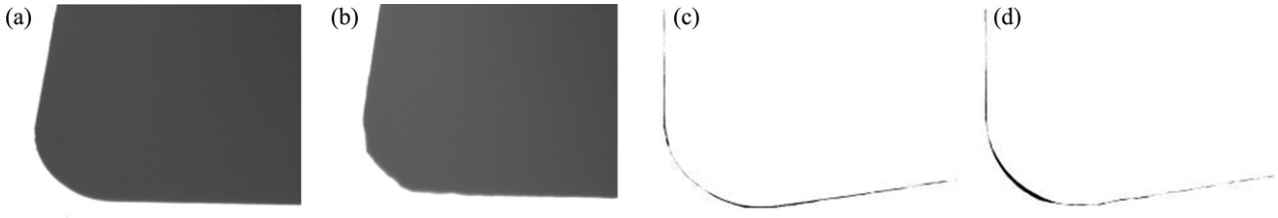

Fig. 10. Images of cutting inserts (a) unworn, (b) example of a worn cutting insert, (c) 0.6 Cr_2O_3 wt% and (d) 0.7 Cr_2O_3 wt%.

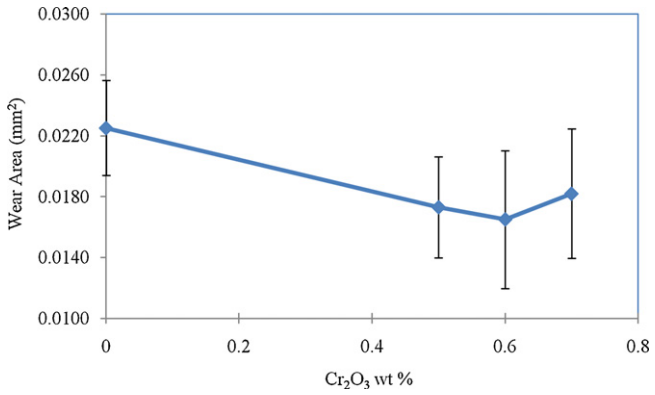

Fig. 11. Wear area of cutting inserts as a function of Cr_2O_3 wt%.

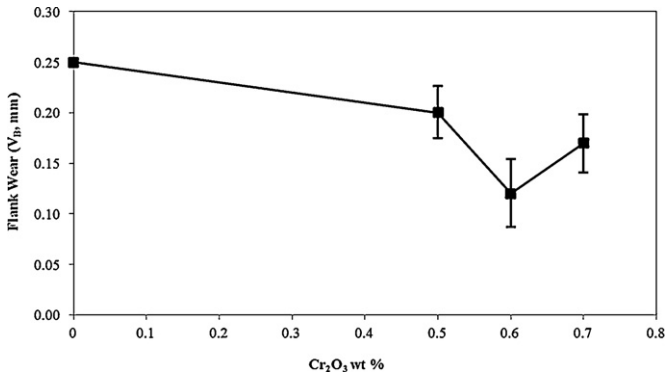

Fig. 12. Flank wear as a function of Cr_2O_3 wt%.

these cutting inserts show high values of Vickers hardness and fracture toughness compared to other samples. The cutting insert with 0 wt% Cr_2O_3 was used as a standard. The cutting insert with 0.6 wt% Cr_2O_3 shows the lowest wear area of 0.0165 mm^2, with 26.70% of improvement compared to ZTA cutting insert with 0 wt% Cr_2O_3, when cutting stainless steel 316L in dry environment.

The life of turning tools particularly of ceramic insert is generally assessed on the basis of flank wear. The flank wear is known to grow systematically with time, cutting temperature and surface roughness. When the average width (V_B) of flank wear reaches a limit, the tool is said to fail and require replacement. For the purpose of research and development, the limiting value of V_B is kept as 0.3 mm. The result of measured flank wear (V_B) is shown in Fig. 12. Similar to the result of nose wear, cutting insert with the addition of 0.6 wt% of Cr_2O_3 shows the lowest flank wear (0.12 mm) compared to cutting insert with 0.5 wt% of Cr_2O_3 and 0.7 wt% of Cr_2O_3. Similar to previous studies, the results of wear area were found to be closely influenced by the result of their mechanical properties [3,4,20], in which the cutting insert with the lowest result of wear shows better results in Vickers hardness and fracture toughness.

4. Conclusion

The microstructure of ZTA composite were significantly affected with the addition of small amount of Cr_2O_3 (~0.6 wt%), the grains becomes larger and acquired a platelike shape. As a result, the fracture toughness was increased from 4.41 MPa $m^{1/2}$ to 4.73 MPa $m^{1/2}$. ZTA cutting insert with 0.6 wt% Cr_2O_3 shows the lowest wear area of 0.0165 mm^2, with 26.70% of improvement compared to ZTA cutting insert with 0 wt% Cr_2O_3, when cutting stainless steel 316L in dry environment.

Acknowledgement

This works was funded by Universiti Sains Malaysia (USM) under the grant 1001/PBAHAN/811074, 1001/PBAHAN/8043043 and the USM Fellowship Scheme. The authors are grateful to Mr. Sharul Ami (USM), Mr. Khairi (USM) and Dr. Shamsul Kamal (Malaysian Mineral Research Centre) for their technical support.

References

[1] Q. Like, L. Xikun, Q. Guanming, M. Weimin, S. Yanbin, Y. Huadong, Journal of Rare Earths 25 (2007) 309–316.
[2] C.P. Dogan, J.A. Hawk, Wear 212 (1997) 110–118.
[3] A.Z.A. Azhar, M.M. Ratnam, Z.A. Ahmad, Journal of Alloys and Compounds 478 (2009) 608–614.
[4] B. Smuk, M. Szutkowska, J. Walter, Journal of Materials Processing Technology 133 (2003) 195–198.
[5] A. Gatto, Journal of Materials Processing Technology 174 (2006) 67–73.
[6] A.K. Dutta, A.B. Chattopadhyaya, K.K. Ray, Wear 261 (2006) 885–895.
[7] B. Mondal, A.B. Chattopadhyay, A. Virkar, A. Paul, Wear 156 (1992) 365–383.
[8] D. Casellas, M.M. Nagl, L. Llanes, M. Anglada, Journal of Materials Processing Technology 143 (2003), 148–115.
[9] N.P. Bansal, S.R. Choi, Processing of Alumina-Toughened-Zirconia Composites in National Aeronautics and Space Administration, John H.Glenn Research Center, Ohio, 2003.
[10] V. Sergo, V. Lughi, G. Pezzotti, E. Lucchini, S. Meriani, N. Muraki, G. Katagiri, S. Lo Casto, T. Nishida, Wear 214 (1998) 264–270.
[11] G. Magnani, A. Brillante, Journal of the European Ceramic Society 25 (2005) 3383–3392.
[12] F. Bondioli, A.M. Ferrari, C. Leonelli, T. Manfredini, L. Linati, P. Mustarelli, Journal of the American Ceramic Society 83 (2000) 2036–2040.
[13] L. Zhang, M. Kuhn, U. Diebold, Surface Science 375 (1997) 1–12.
[14] D.-H Riu, Y.-M. Kong, H.-E. Kim, Journal of the European Ceramic Society 20 (2000) 1475–1481.
[15] K. Niihara, Journal of Materials Science Letters 2 (1983) 221–223.
[16] H. Shahabi, M. Ratnam, The International Journal of Advanced Manufacturing Technology 38 (2008) 718–727.
[17] M.T. Hernandez, M. González, A. De Pablos, Acta Materialia 51 (2003) 217–228.
[18] T. Hirata, K. Akiyama, H. Yamamoto, Journal of the European Ceramic Society 20 (2000) 195–199.
[19] J.K.C. Hao, A.Z.A. Azhar, M.M. Ratnam, Z.A. Ahmad, Materials Science and Technology 26 (2010) 95–103.
[20] A.Z.A. Azhar, H. Mohamed, M.M. Ratnam, Z.A. Ahmad, Journal of Alloys and Compounds 497 (2010) 316–320.